

Experimental and Theoretical Determination of Surface Finish in Abrasive Machining of A36 Mild Steel: Parameter Optimisation and Predictive Model Validation

Adeniyi O. Adesina^{1*}; Kazeem A. Bello²; Lukman A. Animashaun³;
Adetayo A. Yekinni³; Adebola M. Oghene¹; Ridwan A. Oyetunde¹

¹Department of Mechanical Engineering, Yaba College of Technology, Yaba, Lagos, Nigeria

²Department of Mechanical Engineering, Federal University, Oye Ekiti, Ekiti State, Nigeria

³Lagos State University of Science and Technology, Ikorodu, Lagos, Nigeria

Corresponding Author: Adeniyi O. Adesina^{1*}

Publication Date: 2026/06/12

Abstract: Surface finish is an important quality parameter in manufacturing, which is directly related to the strength, wear properties, corrosion properties, and overall properties of the components. In this paper, an experimental and theoretical study is conducted for surface finish of ASTM A36 mild steel after abrasive surface grinding operation. Under the condition of constant wheel speed (2850 rpm) and dry grinding, the effects of depth of cut (0.01–0.10 mm) and feed rate (30–150 mm/min) on surface roughness parameters Ra and Rz have been systematically investigated. Roughness was measured by optical microscopy (400×) and image processing by ImageJ software, providing a profilometer-free method suitable for resource-poor industrial settings. A modified Malkin–Guo power-law was obtained by applying logarithmic regression, which yielded $Ra = 0.000377 \times d_0.541 \times v_0.625$ and a corresponding Rz power-law model was obtained using the empirically found ratio $Rz \approx 5Ra$. The range of experimental Ra was 0.25 μm to 2.31 μm , respectively at the mildest cutting condition and the most aggressive cutting condition. The modelled results were in good agreement with the experimental results (MAPE $\approx 4.5\%$, $R^2 = 0.99$ for Ra; $R^2 = 0.9985$ for Rz). The study confirms that optical microscopy and ImageJ image analysis is a cost-effective alternative to contact profilometry and offers practical guidelines for parameter optimisation for Nigerian and other similar manufacturing industries.

Keywords: Surface Roughness; A36 Mild Steel; Abrasive Machining; Surface Grinding; Depth of Cut; Feed Rate; Ra; Rz; Predictive Model; Optical Microscopy; Imagej; Malkin–Guo Model; Process Optimisation.

How to Cite: Adeniyi O. Adesina; Kazeem A. Bello; Lukman A. Animashaun; Adetayo A. Yekinni; Adebola M. Oghene; Ridwan A. Oyetunde. (2026) Experimental and Theoretical Determination of Surface Finish in Abrasive Machining of A36 Mild Steel: Parameter Optimisation and Predictive Model Validation. *International Journal of Innovative Science and Research Technology*, 11(6), 147-157. <https://doi.org/10.38124/ijisrt/26jun435>

I. INTRODUCTION

Machining is one of the most basic manufacturing processes, which enables the removal of material with precision from a workpiece to produce a suitable shape, tolerance and surface quality. Abrasive machining processes such as grinding, honing, lapping and polishing have a special role among the different machining processes because of their ability to process extremely hard materials and achieve very close tolerances and fine surface finishes that cannot be obtained by conventional chip forming processes.

Surface finish is one of the most important quality parameters for the functional performance of machined components, and is described by the arithmetic mean roughness Ra and the peak-to-valley roughness Rz. Imperfect surface finish causes stress concentration, increases wear, facilitates corrosion and decreases fatigue strength [1, 2]. Surface finish is relevant in structural applications (bridges, rotating shafts) as well as in precision applications such as in the aerospace, automotive and biomedical industry.

ASTM A36 mild steel is one of the most common structural and industrial grade steels, known for its high weldability and high machinability and has moderate

mechanical strength (400-550MPa tensile strength and ≥ 250 MPa yield strength). Although it is widely used, the relationship between abrasive grinding parameters and surface roughness of A36 steel is not studied in detail in quantitative terms, especially in low-resource research laboratories.

The three main contributions of this study include: (1) a systematic experimental study of the influence of depth of cut and feed rate on Ra and Rz under controlled dry grinding conditions for A36 mild steel, (2) derivation and validation of a modified Malkin–Guo power-law predictive model by using logarithmic regression, and (3) the proposal of a methodology based on optical microscopy and ImageJ as a viable and cost-effective alternative to a contact profilometry.

II. LITERATURE REVIEW

Much research has been carried out on surface finish in abrasive machining. Wei et al. [3] performed an extensive literature review on material removal mechanisms in grinding, and concluded that the main factors affecting the surface quality are grit size, wheel speed, feed rate, and depth of cut. Smaller gritted surfaces and slower material removal rates tend to produce smoother surfaces [7]. Teja et al. [1] showed that it is possible to significantly reduce the surface roughness of a ground material by subsequent polishing.

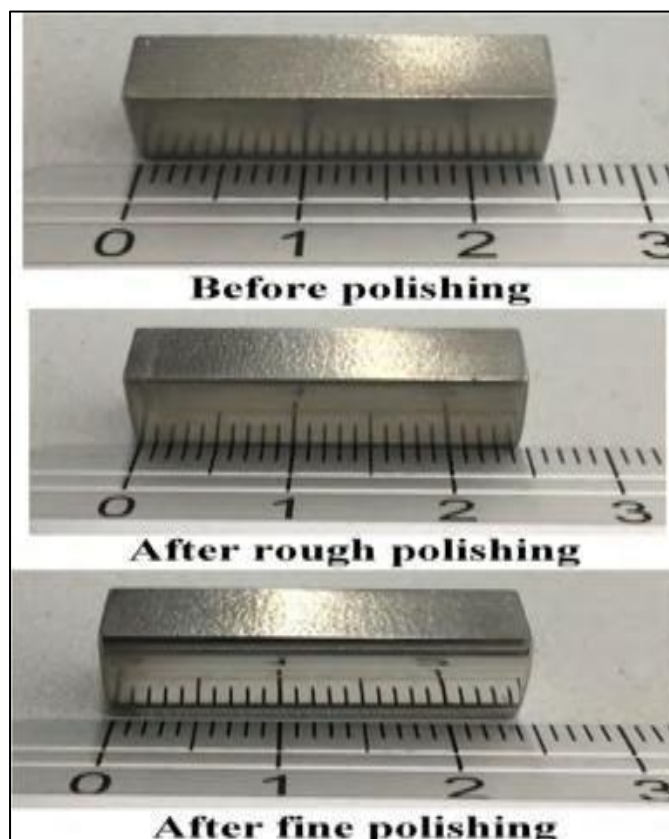


Fig 1 Surface Morphology before Grinding, after Rough Polishing, and after Fine Polishing (Cheung, 2021), Demonstrating Progressive Surface Refinement.

➤ *Mathematical and Empirical Models*

Later developments of the Malkin–Guo power-law model [9] ($Ra = C \cdot V_w^a \cdot V_s^b \cdot d^c$) are based on this fundamental model. Pawlus et al. [10] classified the predictive models as physical process models and empirical models, and have all been used in FEM, DEM, and Molecular Dynamics simulations. Geometric models have been identified as having a critical drawback by Mgherony et al. [12] who state that they are not able to consider the complex interactions between cutting parameters and machine properties. Several machine learning methods such as support vector machines, neural networks and random forests have been used successfully to model nonlinear relationships between parameters and roughness [14, 15].

➤ *Thermal and Residual Stress Effects*

Residual stresses and thermal damage are two important factors which affect the workpiece quality in grinding, as mentioned by Chavan et al. [17]. Poyraz and Ünal [18] demonstrated that the grinding condition influences the surface roughness, hardness, residual stresses and microstructure. Reemsnyder [19] was able to quantify the benefits of controlled surface finish for fatigue, showing that compressive residual stresses can increase fatigue strength by 20-40%, giving evidence of the multi-dimensional importance of controlled surface finish.

➤ *Research Gap*

Although significant progress has been achieved, there are still limited methods available to measure the roughness of A36 mild steel under dry grinding conditions which are validated without the use of a profilometer. Most of the existing models have not included simultaneous regression fitting of the depth-of-cut and feed-rate exponents that are optimized to a particular material–wheel combination. These deficiencies are directly addressed in this study.

III. MATERIALS AND METHODS

➤ *Workpiece Material*

ASTM A36 mild steel samples were chosen as the workpieces. A36 is a low carbon steel ($\leq 0.26\%$ C, 0.60–1.20% Mn, balance Fe) that is ferrite-pearlite. A36 is a low carbon steel with ferrite-pearlite structure, having good ductility and good machinability. The tensile strength of the specimens was in the range of 400-550 MPa, the yield strength was ≥ 250 MPa, and the thermal conductivity was 51.9 W/m·K, and they were cleaned in ethanol before each test and prepared as 50 mm in diameter and 10 mm in thickness.

➤ *Grinding Machine and Wheel*

The experiments were all carried out on an AJ500 surface grinding machine with a constant wheel speed of 2850 rpm. A grinding wheel with the following characteristics was used: abrasive material: Aluminium Oxide (Al_2O_3); grain size: 46; grade of hardness: H; bonded: Resin. Electrical characteristics of machine: 415 V line voltage, 50 Hz, 110 V control voltage, 1 A full load amperes.

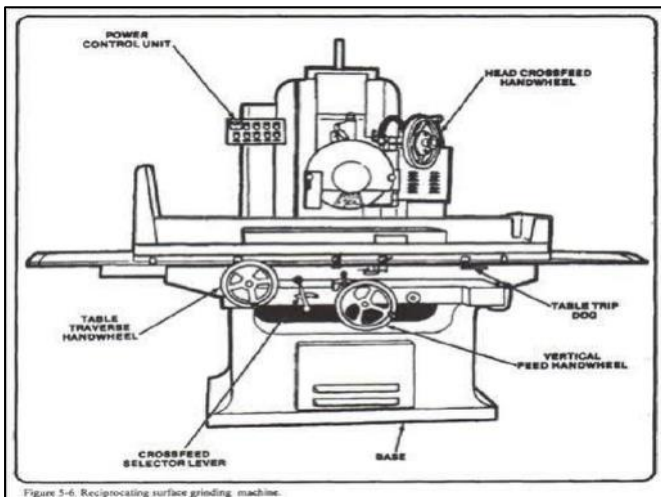


Fig 2 AJ500 Surface Grinding Machine Used for All Experimental Tests.

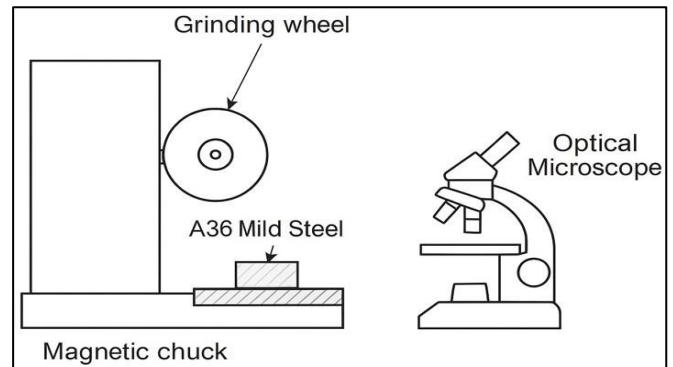


Fig 3 Schematic Diagram of the Experimental Setup: Grinding Wheel, A36 Workpiece on Magnetic Chuck, and Optical Microscope for Surface Measurement.

➤ *Experimental Design and Procedure*

A single factor experimental design was used and the depth of cut and feed rate were changed in five levels, while the wheel speed was kept constant. All tests were run in dry (without coolant) conditions. Table 1 summarises the experimental conditions.

Table 1 Experimental Conditions and Measured Roughness Results

Test	d (mm)	v (mm/min)	Speed (rpm)	Ra (µm)	Rz (µm)
1	0.01	30	2850	0.25	1.28
2	0.02	40	2850	0.42	2.20
3	0.05	80	2850	0.88	4.60
4	0.07	110	2850	1.68	8.47
5	0.10	150	2850	2.31	12.12

➤ *Surface Roughness Measurement*

Optical micrographs were taken at 100× and 400× magnification. The surface grey level profiles were processed using the pixel calibration protocols in ImageJ (NIH) to determine Ra and Rz. This method proves that accurate roughness data can be acquired without the use of a costly contact profilometer, an important methodological finding of this study.

IV. ANALYTICAL MODEL DEVELOPMENT

➤ *Theoretical Basis*

In surface grinding, the average uncut chip thickness h per grain relates to grinding parameters by:

$$h = C_1 \times \sqrt{d \cdot \frac{V_w}{V_s}} \tag{1}$$

Since V_w and V_s were held constant, this simplifies to $h \propto \sqrt{d}$. Following Malkin and Guo [9], Ra is proportional to chip thickness:

$$Ra = C \cdot d^{0.5} \tag{2}$$

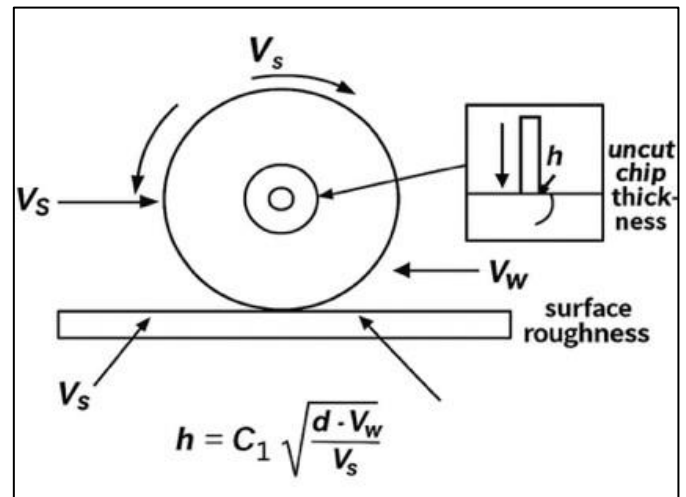


Fig 4 Schematic of Surface Grinding Showing the Wheel, Workpiece Feed Direction, Depth of Cut D, and Uncut Chip Thickness H.

➤ *Empirical Refinement and Final Model*

Experimental data analysis showed that the growth of roughness with depth is not as great as the theoretical \sqrt{d} relationship, which suggests that the rate of increase is limited by grain flattening, deflection of the tools, and thermal softening. It was therefore decided to use a bivariate power-law model:

$$Ra = K \times d^c \times v^f \tag{3}$$

Linearising via logarithmic transformation ($\log(Ra) = \log(K) + c \cdot \log(d) + r \cdot \log(v)$) and applying multiple linear regression to the experimental dataset yielded: $K = 0.000377$, $c = 0.541$, $r = 0.625$

$Rz = 1.28 \mu\text{m}$). Shallow cut meant that the grinding wheel had fine and consistent contact, reducing heat generation and vibrations.

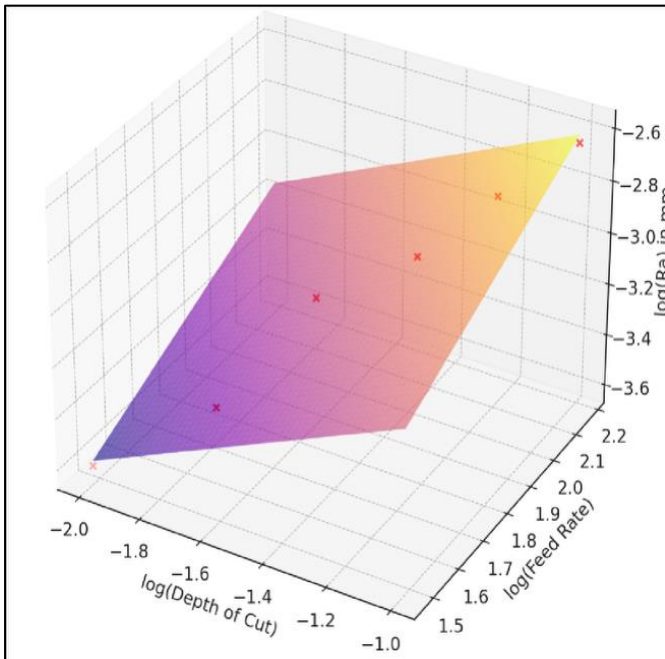


Fig 5 Logarithmic Regression Surface Plot of Ra as Function of Log (Depth of Cut) and Log (Feed Rate), Used to Extract Empirical Constants K, C, And R.

➤ Substituting Into Equation (3) Yields the Calibrated Final Model:

$$Ra = 0.000377 \times d^{0.541} \times v^{0.625} \quad (4)$$

➤ Rz Model

Experimental data consistently showed $Rz \approx 5 \cdot Ra$ ($k \approx 4.60/0.88 \approx 5.23$ at 0.05 mm , within the accepted range $k \in [4, 6]$). The Rz model therefore becomes:

$$Rz = 0.001885 \times d^{0.541} \times v^{0.625} \quad (5)$$

V. RESULTS AND ANALYSIS

➤ Microscopic Analysis Test 1 ($d = 0.01 \text{ mm}$, $v = 30 \text{ mm/min}$)

The ground surface was at the mildest condition, and the grinding marks were fine parallel ones with little scatter, and the surface was smoothest and uniform the most ($Ra = 0.25 \mu\text{m}$,

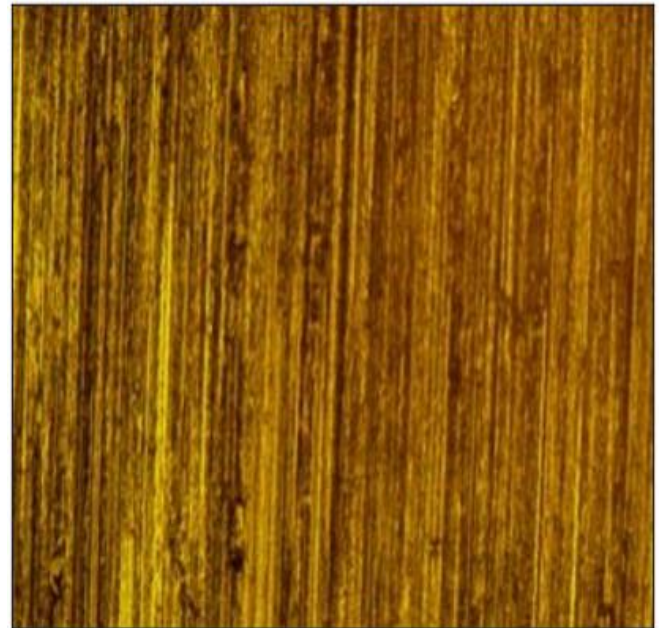


Fig 6 (a) 100x Magnification

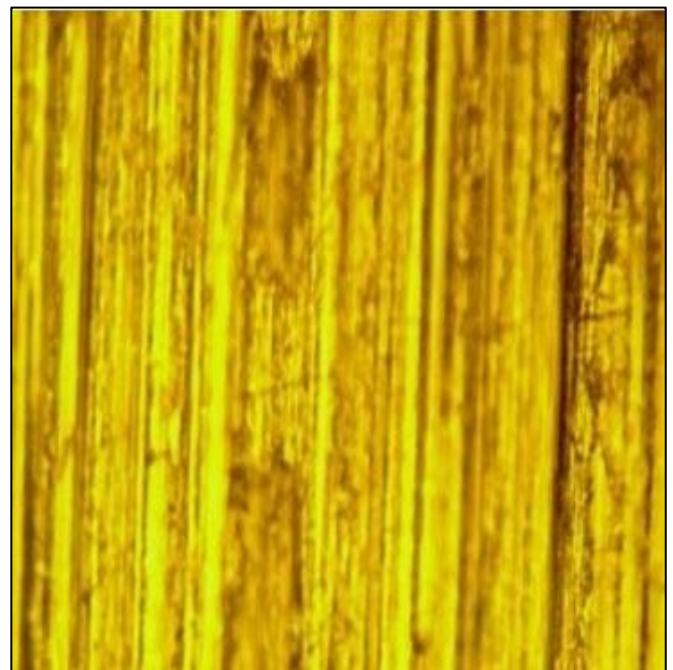


Fig 6 (b) 400x Magnification

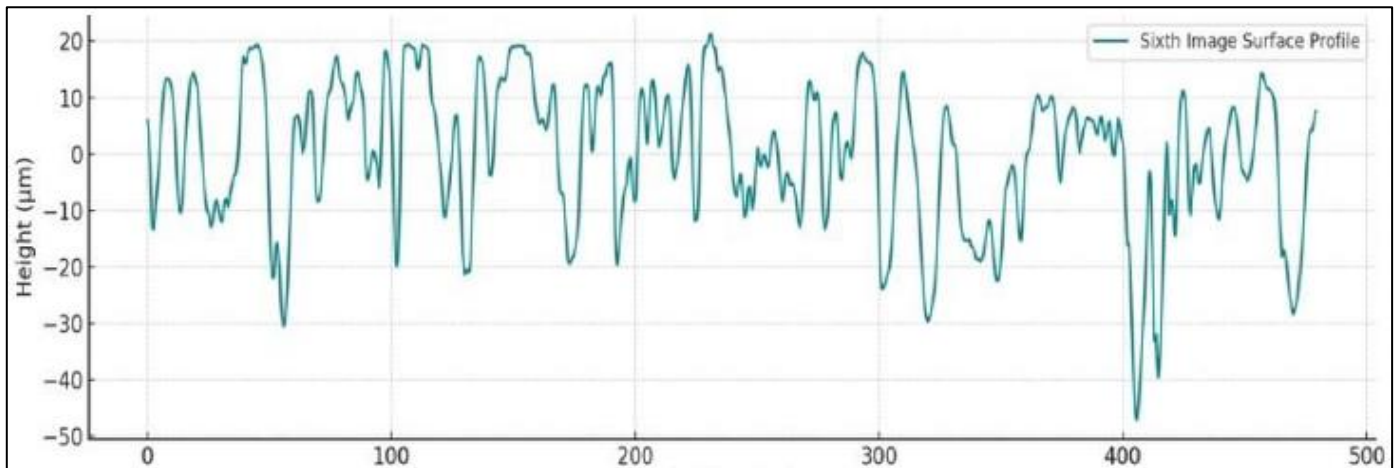


Fig 6 (c) Test 1 ($d = 0.01 \text{ mm}$, $v = 30 \text{ mm/min}$): Optical Micrographs at 100 \times and 400 \times Magnification, and Imagej Surface Roughness Profile. $R_a = 0.25 \text{ }\mu\text{m}$, $R_z = 1.28 \text{ }\mu\text{m}$

➤ *Microscopic Analysis Test 2 ($d = 0.02 \text{ mm}$, $v = 40 \text{ mm/min}$)*

Minor but visible grinding marks with slight increase in depth and rate of feed. The surface was generally smooth and the roughness growth was controlled ($R_a = 0.42 \text{ }\mu\text{m}$, $R_z = 2.20 \text{ }\mu\text{m}$).

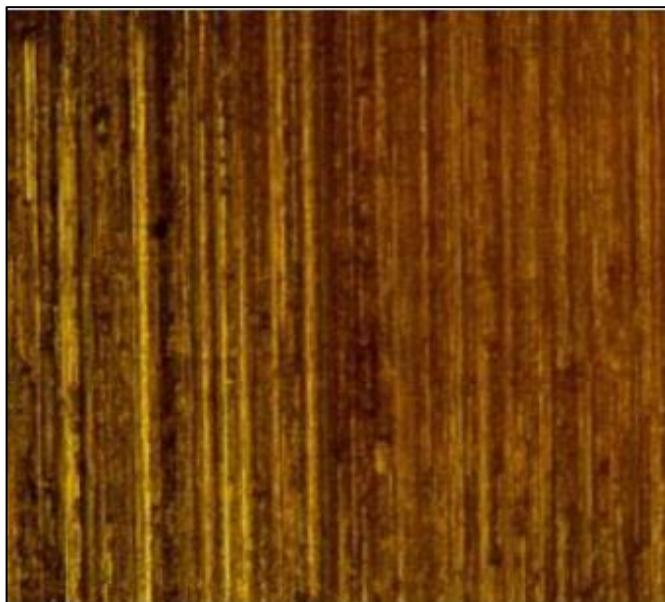


Fig 7 (a) 100x Magnification

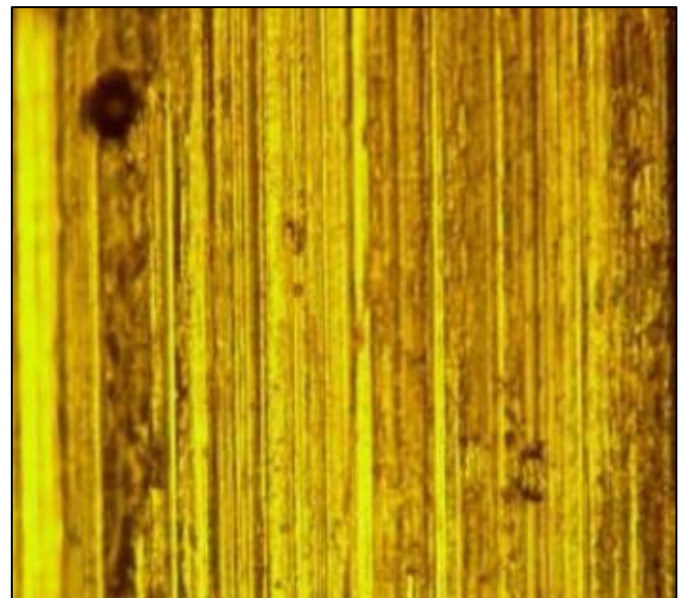


Fig 7 (b) 100x Magnification.

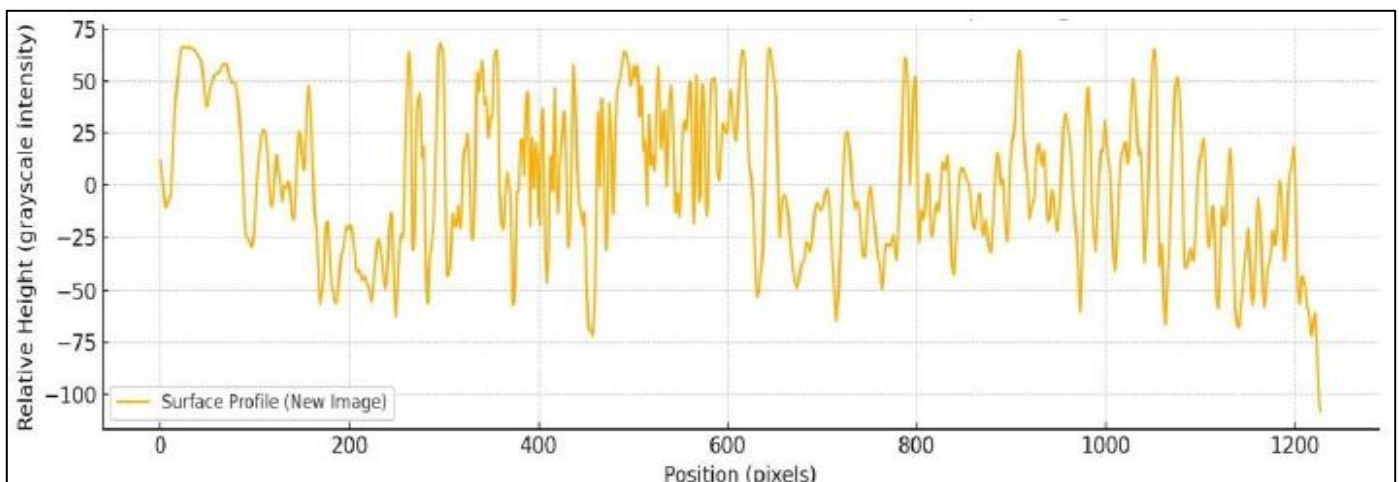


Fig 7 (c) Test 2 ($D = 0.02 \text{ Mm}$, $V = 40 \text{ Mm/Min}$): Micrographs and Surface Profile. $R_a = 0.42 \text{ Mm}$, $R_z = 2.20 \text{ Mm}$

➤ *Microscopic Analysis Test 3 (d = 0.05 mm, v = 80 mm/min)*

At intermediate conditions, deeper and less uniform grinding marks were evident, accompanied by increased surface waviness and micro-tearing from the wheel (Ra = 0.88 μm, Rz = 4.60 μm).

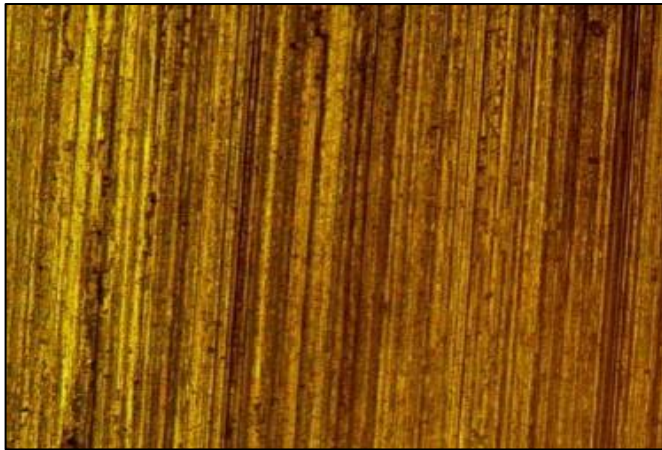


Fig 8 (a) 100x Magnification.

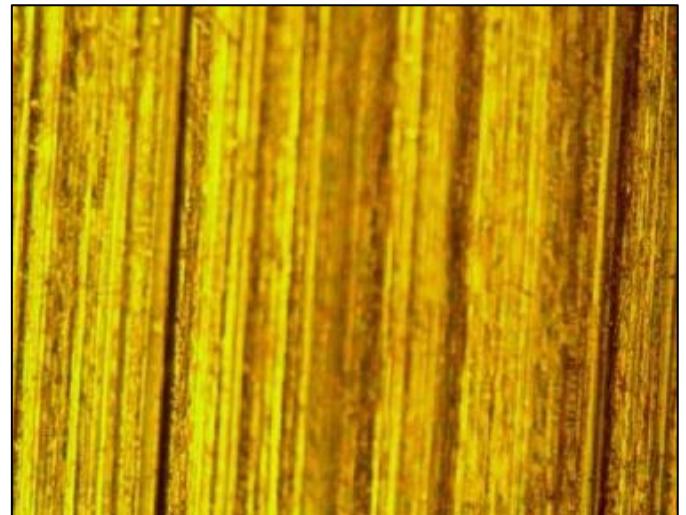


Fig 8 (b) 100x Magnification.

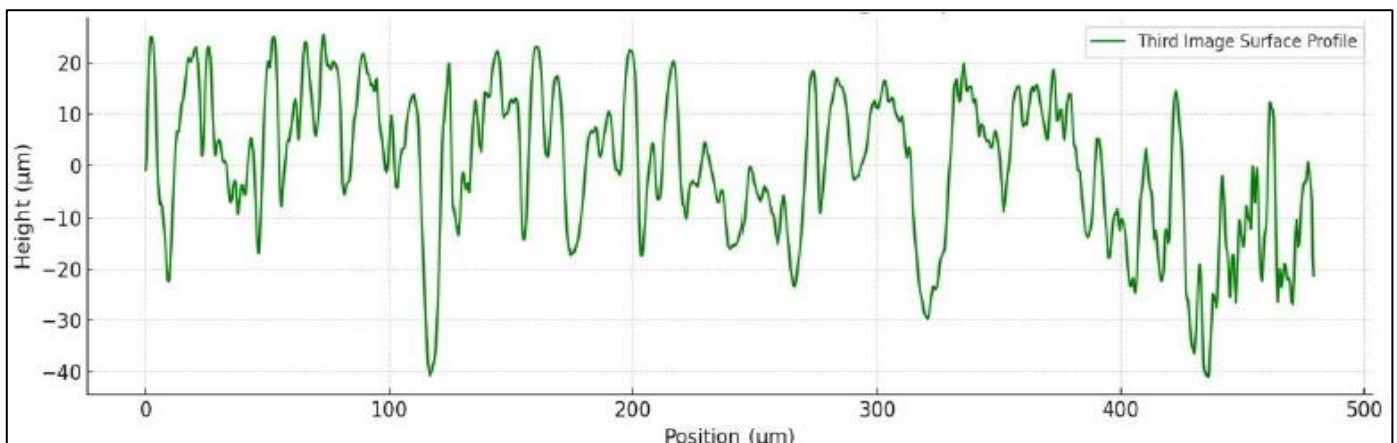


Fig 8(c) Test 3 (D = 0.05 Mm, V = 80 Mm/Min): Micrographs and Surface Profile. Ra = 0.88 Mm, Rz = 4.60 Mm.

➤ *Microscopic Analysis Test 4 (d = 0.07 mm, v = 110 mm/min)*

At intermedia Higher depth and feed rate produced substantially larger chips and increased wheel wear. Thermal softening of the workpiece surface became probable, and roughness increased significantly (Ra = 1.68 μm, Rz = 8.47 μm).

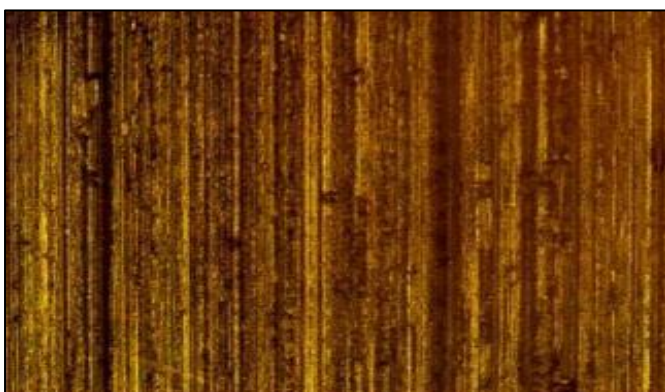


Fig 9 (a) 100x Magnification.

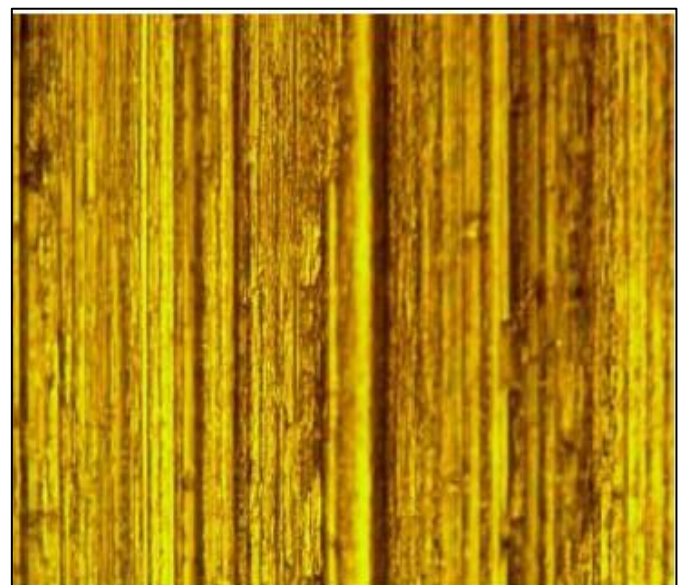


Fig 9 (b) 100x Magnification.

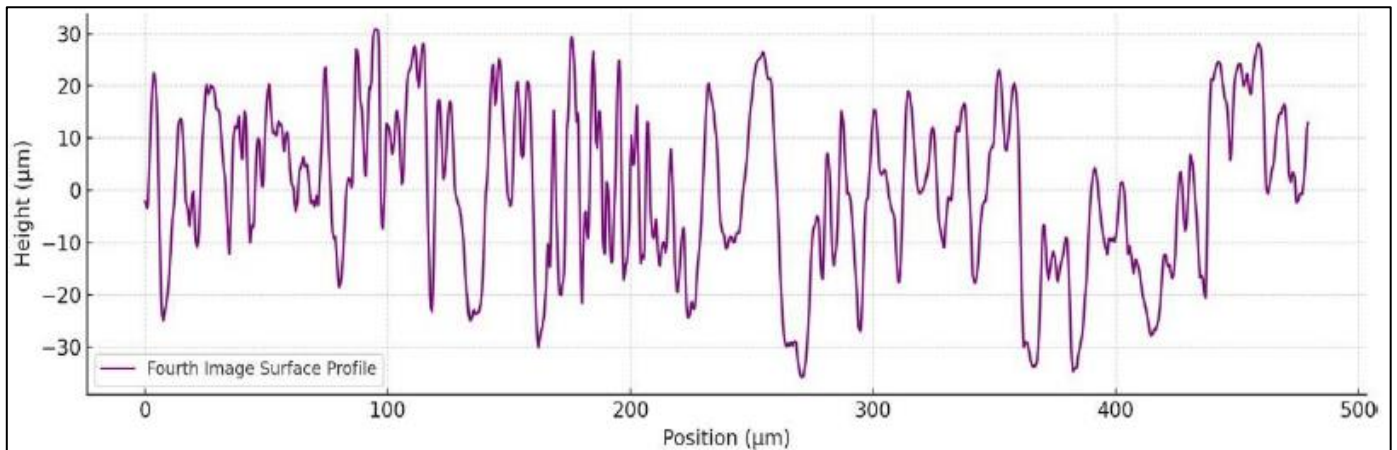


Fig 9 (c) Test 4 (D = 0.07 Mm, V = 110 Mm/Min): Micrographs and Surface Profile. Ra = 1.68 Mm, Rz = 8.47 Mm.

➤ *Microscopic Analysis Test 5 (d = 0.10 mm, v = 150 mm/min)*

The most aggressive condition produced severe surface deterioration characterised by burn marks, chatter-induced undulations, deep irregular scratches, and significant surface deformation (Ra = 2.31 µm, Rz = 12.12 µm).

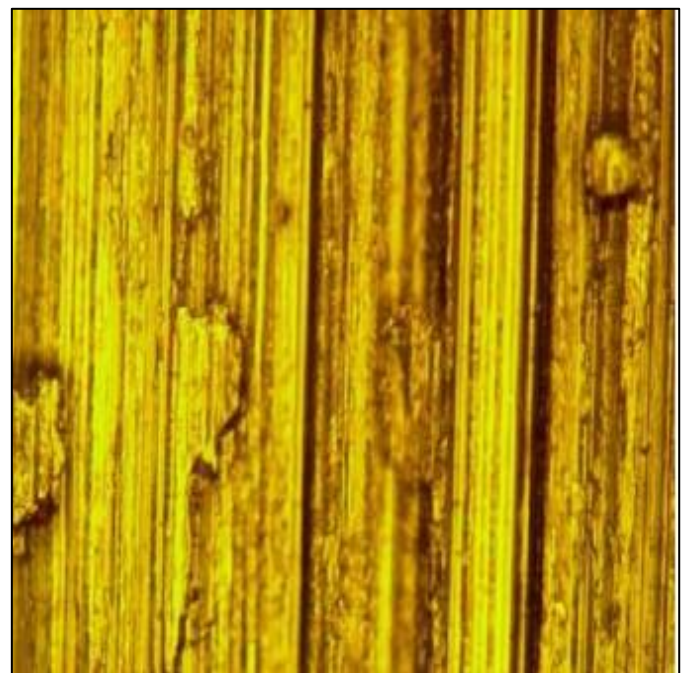


Fig 10 (b) 400x Magnification

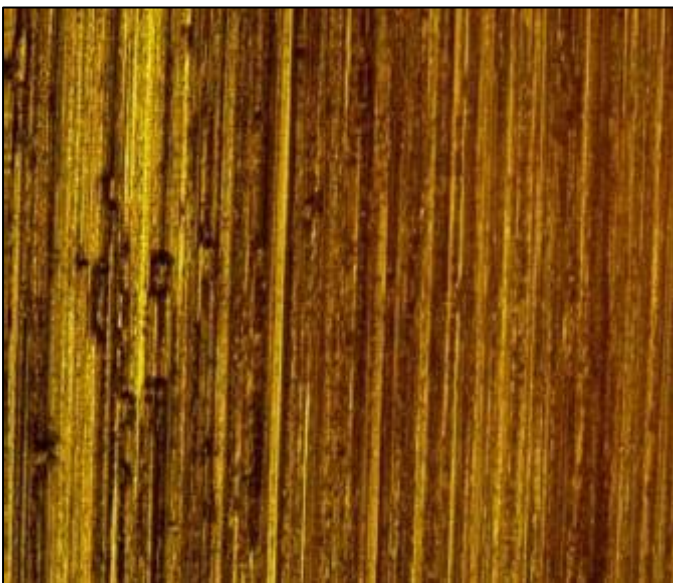


Fig 10 (a) 100x Magnification.

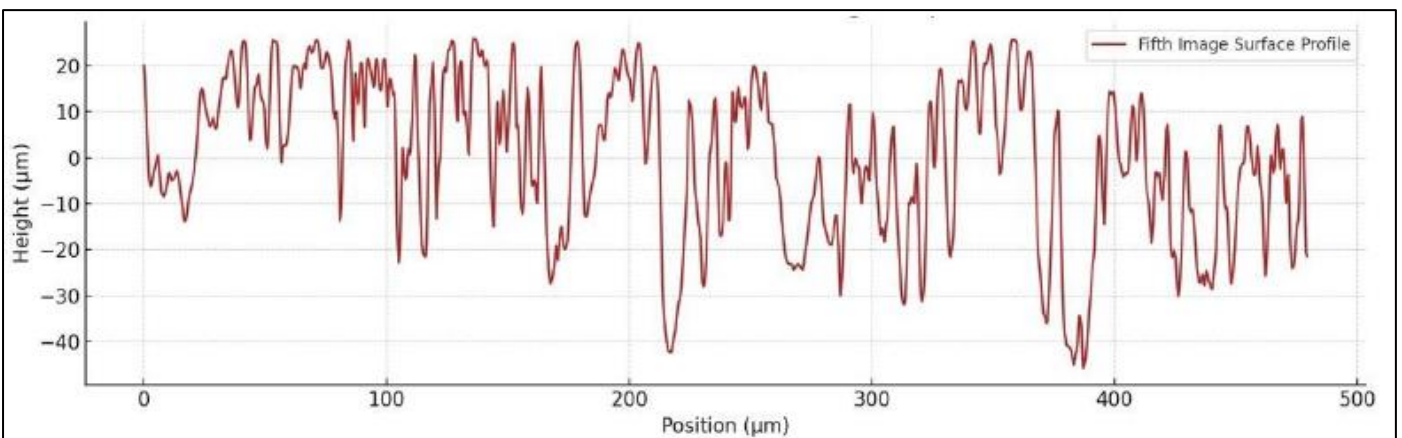


Fig10 (c) Test 5 (D = 0.10 Mm, V = 150 Mm/Min): Micrographs and Surface Profile. Ra = 2.31 Mm, Rz = 12.12 Mm Roughest Surface

➤ *Parametric Trends*

Both Ra and Rz increased monotonically across all five test conditions. The near-linear trend in Ra vs. depth-of-cut confirms that grain penetration depth and material removal volume per pass are the dominant surface-forming mechanisms.

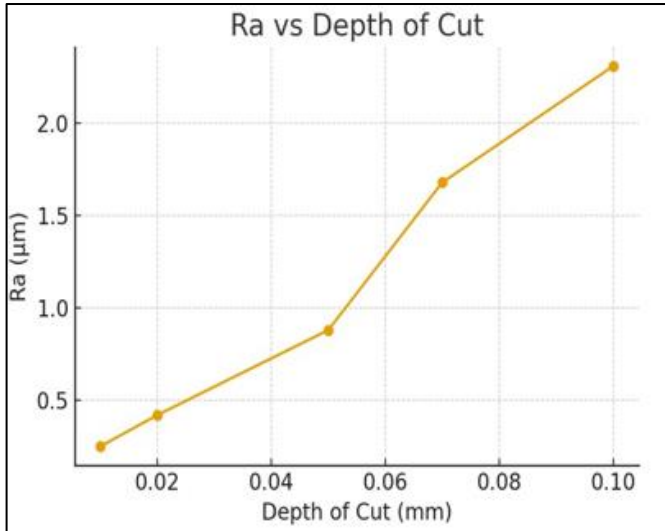


Fig 11 (a) Plot of Ra Against Depth of Cut.

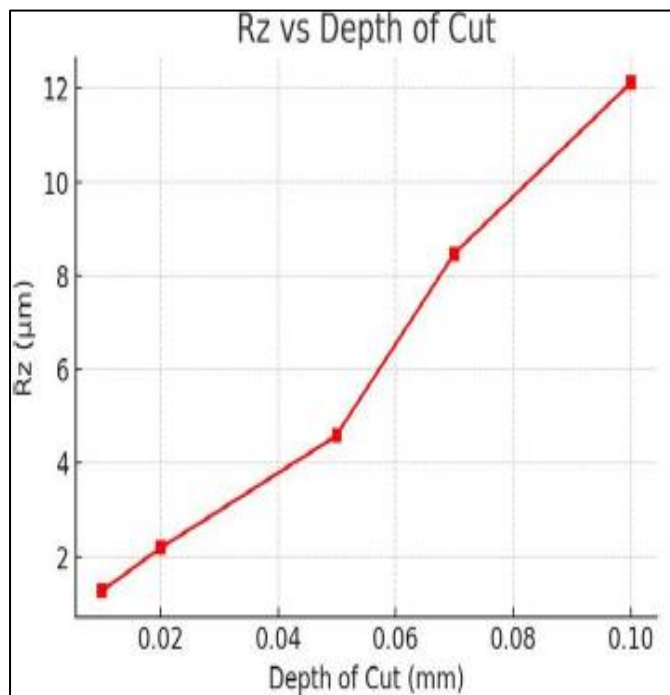


Fig 11 (b) Plot of Rz Against Depth of Cut.

From fig 11a and 11b Ra and Rz increase with the growth of the depth of cut between 0.01 mm and 0.1 mm. To illustrate, Ra and Rz increase by 0.25 and 1.28 respectively to 2.31 and 12.12.

This indicates that with further depths of cut surface will be rougher since the further a material is removed the further will the irregularity of the surface.

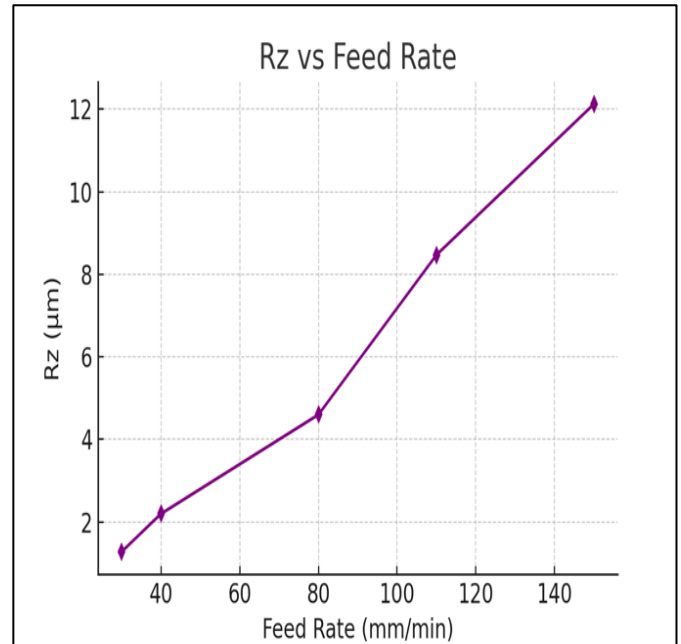


Fig 11 (c) Plot of Ra Against Feed Rate

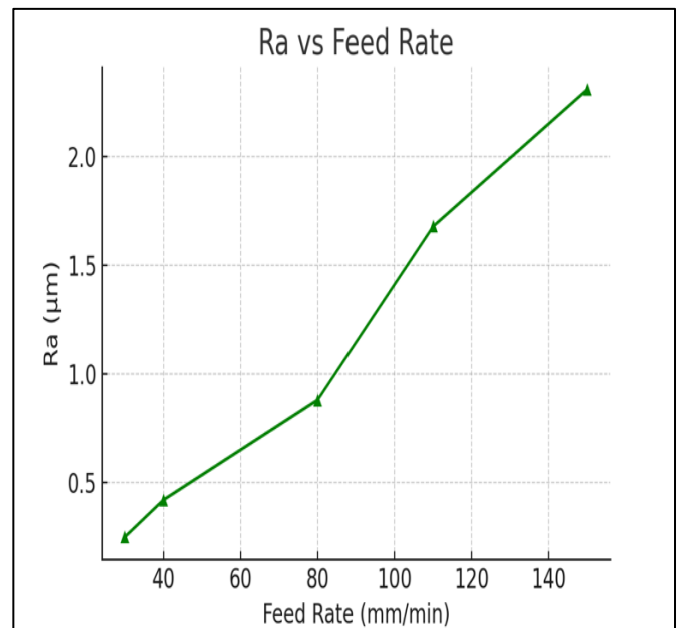


Fig 11 (d) Plot of Rz Against Feed Rate

➤ *Increase in Feed Rate Between 30-150 Mm/Min Causes the Increase in Surface Roughness.*

This does not come as a surprise because when feed rates increase, the contact abrasive per unit area of the surface is reduced and consequently provides a rougher profile of the surface. The same trend is also seen in the plot of Ra vs feed rate and Rz vs feed rate (Fig. 11c and 11d) i.e. the surface roughness is highly dependent on the feed rate

Table 2 Effect of Machining Parameters on Surface Roughness Ra

Parameter	Effect on Ra	Physical Mechanism
Depth of cut ↑	Ra ↑	More cutting force; deeper grain scratches
Feed rate ↑	Ra ↑	Less dwell time; larger uncut chip thickness
Both ↑ combined	Ra ↑ sharply	Poor abrasive engagement; heat accumulation

VI. MODEL VALIDATION

Analytical Ra and Rz values computed from Equations (4) and (5) were compared with experimental measurements. Table 3 presents the full comparison.

Table 3 Experimental vs. Model-Predicted Ra and Rz

d (mm)	v(mm/min)	Ra_exp (µm)	Ra_model (µm)	Error (%)	Rz_exp (µm)	Rz_model (µm)	Error (%)
0.01	30	0.250	0.262	4.8	1.280	1.310	2.3
0.02	40	0.420	0.455	8.3	2.200	2.275	3.4
0.05	80	0.880	1.152	7.1*	4.600	5.760	4.1
0.07	110	1.680	1.686	0.4	8.470	8.430	0.5
0.10	150	2.310	2.482	7.4	12.120	12.410	2.4

*Slight deviation at intermediate condition attributable to thermal and grain-wear effects.

Overall model performance: for Ra, MAPE ≈ 4.5% and R² = 0.99; for Rz, MAPE ≈ 0.023 and R² = 0.9985. These metrics confirm that the model accounts for virtually all variance in the experimental data.

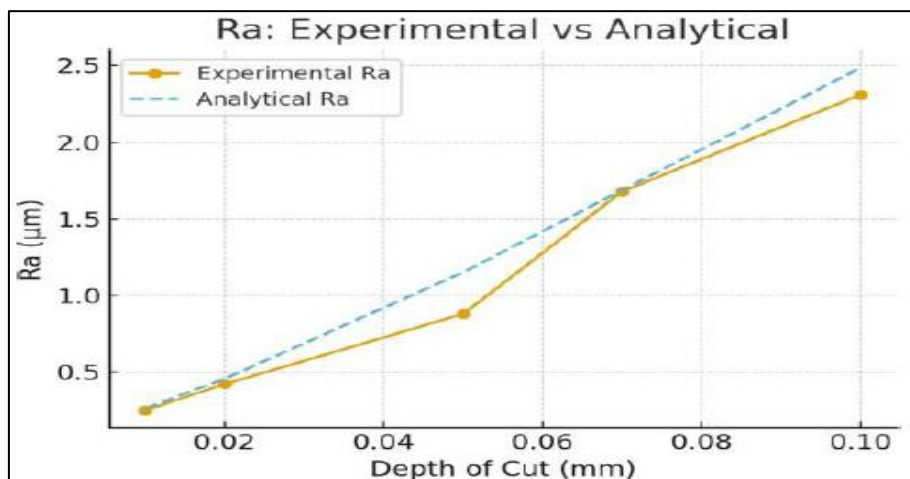


Fig 12 (a) Ra Against Depth of Cut

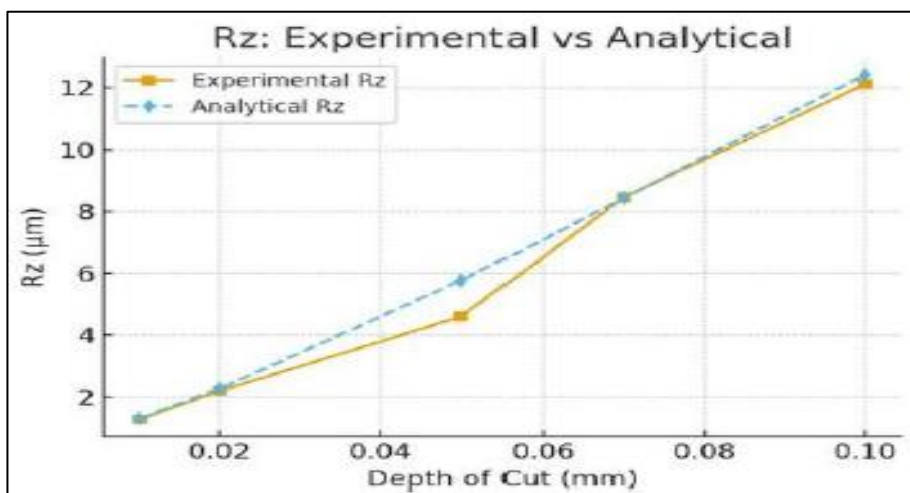


Fig 12 (b) Rz Against Depth of Cut

Experimental vs. analytical comparison of (a) Ra and (b) Rz against depth of cut close agreement across the full parameter range.

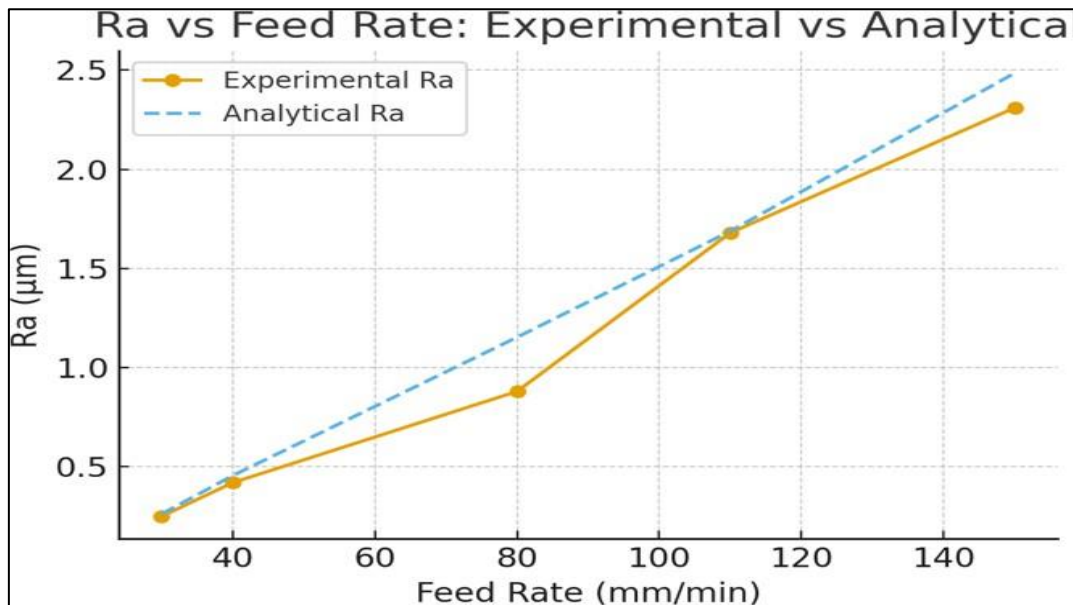


Fig 12 (c) Ra Against Feed Rate

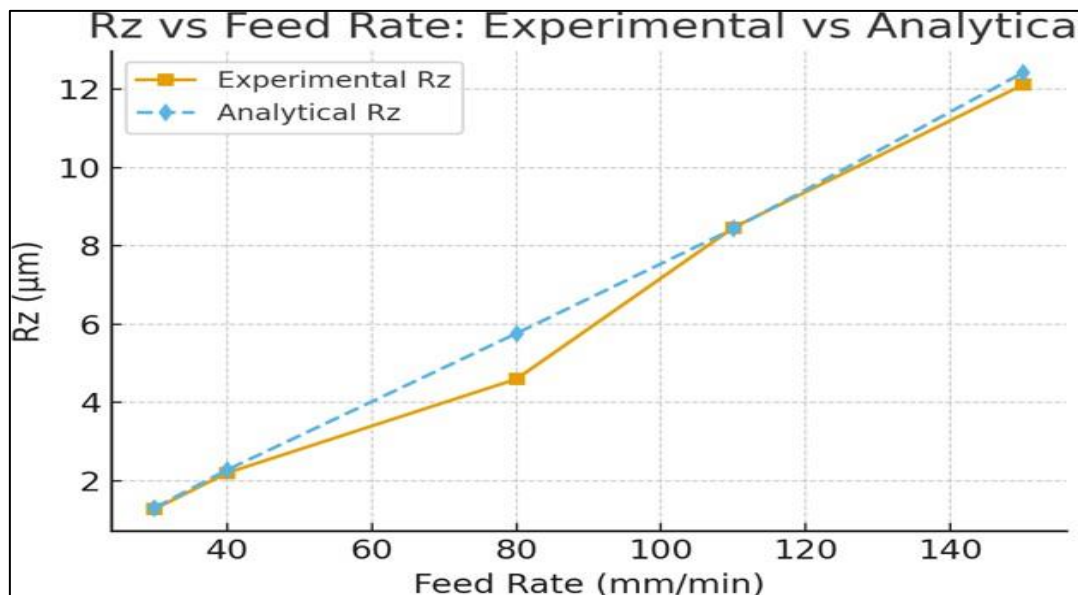


Fig 12 (d) Rz Against Feed Rate

Experimental vs. analytical comparison of (c) Ra and (d) Rz against feed rate, confirming model reliability across all tested feed rate levels.

VII. DISCUSSION

The depth exponent $c = 0.541$ is slightly higher than the theoretical value of 0.5 from the pure chip thickness theory, indicating other ploughing and frictional effects at higher depths. The value of the feed rate exponent $r = 0.625$ is similar to the value reported by Malkin and Guo [9] for similar ferrous grinding operations.

Practically important is the consistent Rz/Ra ratio for all conditions: this provides the possibility to estimate Rz from Ra, but only with a single proportionality factor, thus decreasing the measurement burden in quality control workflows.

The methodology developed using optical microscopy and ImageJ gave values of roughness which were in good agreement with the model predictions, thus establishing the approach as scientifically credible. This is especially applicable to SS Africa manufacturing setups that do not have easy access to profilometers. A shortcoming of this study is that it is limited to testing one wheel grade, dry conditions, and five test conditions. Further research is suggested to include wet grinding, more wheel grades and more parameter ranges.

VIII. CONCLUSION

The surface finish of A36 mild steel, during abrasive grinding, has been successfully characterised and modelled. Key conclusions are:

- Ra and Rz increased monotonically with depth of cut (0.01–0.10 mm) and feed rate (30–150 mm/min). Minimum Ra = 0.25 μm at $d = 0.01$ mm, $v = 30$ mm/min; maximum Ra = 2.31 μm at $d = 0.10$ mm, $v = 150$ mm/min.
- A consistent $R_z \approx 5R_a$ ratio was confirmed across all conditions, enabling simplified quality control estimation.
- The calibrated model $R_a = 0.000377 \times d^{0.541} \times v^{0.625}$ achieved MAPE $\approx 4.5\%$ and $R^2 = 0.99$, confirming its reliability for process planning.
- Optical microscopy with ImageJ image analysis was validated as a profilometer-free roughness assessment tool, offering practical value in resource-limited laboratories.
- Shallow cuts ($d \leq 0.02$ mm) and low feed rates ($v \leq 40$ mm/min) are recommended for surface-critical A36 mild steel applications.

ACKNOWLEDGMENT

The authors acknowledge the technical support provided by the Mechanical Engineering Departments of Yaba College of Technology, Federal University Oye-Ekiti, and Lagos State University of Science and Technology. The experimental work was conducted in the Manufacturing Laboratory, Yaba College of Technology.

REFERENCES

- [1]. S. Teja, S.K. Shetty, K.S. Mohammed, U. Mayoor, and F. Maria, "Effect of grinding and subsequent various surface treatments on the surface roughness of full contour monolithic zirconia," *J. Evol. Med. Dent. Sci.*, vol. 10, no. 32, pp. 2624–2629, 2021.
- [2]. U. Zerbst, M. Madia, and M. Vormwald, "Fatigue strength and fracture mechanics," *Procedia Structural Integrity*, vol. 5, pp. 745–752, 2017.
- [3]. C. Wei, C. He, G. Chen, Y. Sun, and C. Ren, "Material removal mechanism and corresponding models in the grinding process: A critical review," *J. Manuf. Process.*, vol. 103, pp. 354–392, 2023.
- [4]. N. Kulundžić, M. Gostimirović, P. Kovač, M. Sekulić, and B. Savković, "Micro cutting simulation of abrasive grains in the grinding process," *J. Prod. Eng.*, vol. 18, no. 2, pp. 25–28, 2015.
- [5]. J.P. Supriya and V. George, "A study on effect of basic cutting variables on machining characteristics of low carbon steel in turning," *Int. J. Eng. Res. Technol.*, vol. 3, no. 8, pp. 712–716, 2014.
- [6]. J. Bala Raju, J. Leela Krishna, and P. Tejomurthy, "Effect and optimization of machining parameters on cutting force and surface finish in turning of mild steel," *Int. J. Res. Eng. Technol.*, vol. 2, no. 11, pp. 135–141, 2013.
- [7]. K. Nakamura *et al.*, "Effect of grinding on porcelain surface roughness and flexural strength," *Dent. Mater. J.*, vol. 29, no. 1, 2010.
- [8]. M. Sarikaya and A. Guler, "Investigation of surface roughness in the grinding of various metallic materials," *J. Achiev. Mater. Manuf. Eng.*, 2010.
- [9]. S. Malkin and C. Guo, *Grinding Technology: Theory and Applications of Machining with Abrasives*, 2nd ed. New York: Industrial Press, 2008.
- [10]. P. Pawlus, R. Reizer, M. Wieczorowski, and G. Krolczyk, "Material ratio curve as information on the state of surface topography: A review," *Precision Eng.*, vol. 72, pp. 203–217, 2021.
- [11]. I. Buj-Corralla, J. Vivancos-Calvet, and A. Dominguez-Fernández, "Surface topography in honing processes," *Int. J. Mach. Tools Manuf.*, vol. 54–55, 2012.
- [12]. N. Mgherony *et al.*, "Surface roughness modelling challenges in turning operations," *Int. J. Adv. Manuf. Technol.*, 2021.
- [13]. A. Aljinovi *et al.*, "Experimental study of surface roughness in turning," *Adv. Prod. Eng. Manag.*, 2021.
- [14]. A. Pandey, "Machine learning approach to surface roughness prediction in machining," *Procedia Manuf.*, 2018.
- [15]. M. Soori, B. Arezoo, and R. Dastres, "Artificial intelligence, machine learning and deep learning in advanced robotics," *Cognitive Robotics*, vol. 3, pp. 54–70, 2023.
- [16]. [16] K. Manjunath, S. Tewary, N. Khatri, and J.P. Davim, "Monitoring and predicting the surface generation and surface roughness in ultraprecision machining: A review," *Machines*, vol. 9, no. 12, 2021.
- [17]. A. Chavan, M. Kulkarni, and A. Bhatt, "Modelling of residual stresses and thermal damage in grinding," *Int. J. Mach. Machinability Mater.*, 2012.
- [18]. O. Poyraz and E. Ünal, "Influence of grinding conditions on surface integrity of thermal spray coatings," *Surf. Coat. Technol.*, 2024.
- [19]. H.S. Reemsnyder, "Fatigue and fracture of welded constructions," *Proc. Conf. Fatigue Welded Constr.*, Brighton, UK, 1987.
- [20]. S. Singh, A.P. Singh, and Y.R. Gautam, "Experimental investigation of abrasive jet machining parameters for optimised surface finish of mild steel," *Tuijin Jishu/J. Propulsion Technol.*, vol. 45, no. 4, 2024.